SPE 118944

A Multi-Continuum Model for Gas Production in Tight Fractured Reservoirs

Yu-Shu Wu, SPE, Colorado School of Mines; George Moridis, SPE, Lawrence Berkeley National Laboratory; Baojun Bai, SPE, Missouri University of Science and Technology; Keni Zhang, SPE, Lawrence Berkeley National Laboratory

This paper was prepared for presentation at the 2009 SPE Hydraulic Fracturing Technology Conference held in The Woodlands, Texas, USA, 19–21 January 2009.

Abstract

Tight gas reservoirs are characterized by single-phase (gas) or two-phase (gas and liquid) flow in extremely low-permeability, highly heterogeneous porous/fractured, and stress-sensitive rock. Gas flow in such tight formations is further complicated by other co-existing processes, such as Klinkenberg effect, non-Newtonian or non-Darcy flow behavior, due to strong interaction between fluid molecules and solid materials within tiny pores, or micro- and macro- fractures. Because of the low permeability in tight rock, the traditional double-porosity model may not be applicable for handling fracture-matrix interaction of gas flow in these reservoirs. In this work, we present a generalized mathematical model for simulating multiphase flow of gas in tight, porous/fractured reservoirs using a more general, multi-continuum modeling approach. The model incorporates the following processes: (1) Klinkenberg effect, (2) non-Newtonian behavior (i.e., threshold pressure gradient for flow to occur); (3) non-Darcy flow with inertial effects; and (4) rock deformation due to changes in the stress field. We propose to explicitly separate effects of rock mechanical deformation and molecular interaction between fluids and rock materials. The former effect is included using the intrinsic permeability and porosity relations, while the latter is accounted for by an apparent viscosity for non-Newtonian, non-Darcy's behavior, or a modified permeability for Klinkenberg effect

The proposed mathematical model has been implemented into a multiphase, multidimensional reservoir simulator. In the numerical model, specifically, a control-volume, integral finite-difference method is used for spatial discretization with an unstructured grid, and a first-order finite-difference scheme is adapted for temporal discretization of governing two-phase flow equations in tight gas reservoirs. The resulting discrete nonlinear equations are solved fully implicitly by Newton iteration. The numerical scheme has been verified against analytical solutions with Klinkenberg effect, non-Newtonian or non-Darcy flow, and flow in deformable fractured rock in our previous studies. The model's application to actual tight gas reservoirs is an on-going research project.

Introduction

Since the 1960s, significant progress has been made in modeling of flow and transport processes in fractured rock. Driven by the increasing need to develop petroleum, geothermal, and other natural underground energy resources and to study the problem of subsurface contamination, researchers have developed several numerical modeling approaches and techniques (Barenblatt et al. 1960; Warren and Root, 1963; Kazemi, 1969; Pruess and Narasimhan, 1985). Numerical modeling approaches, developed in the past few decades, rely in general on continuum approaches and involve developing conceptual models, incorporating the geometrical information of a given fracture-matrix system, setting up mass and energy conservation equations for fracture-matrix domains, and then solving discrete nonlinear algebraic equations. The key issue for simulating flow in fractured rock, however, is how to handle fracture-matrix interaction under different flow conditions. To model fracture-matrix interaction in fractured porous media, investigators have developed and applied many different conceptual models and modeling approaches for dealing with fracture-matrix interaction, including: (1) an explicit discrete-fracture and matrix model (e.g., Snow, 1965), (2) the dual-continuum method, including double- and multiporosity, dual-permeability, or the more general "multiple interacting continua" (MINC) method (Barenblatt et al. 1960; Warren and Root, 1963; Kazemi, 1969; Pruess and Narasimhan, 1985; Wu and Pruess, 1988), and (3) the effective-continuum method (ECM) (Wu, 2000).

The explicit discrete-fracture approach is, in principle, a more rigorous model. However, the application of this method to field studies is still limited because of the computational intensity involved as well as the lack of detailed knowledge of

fracture and matrix geometric properties and their spatial distributions in reservoirs. On the other hand, the dual-continuum method is conceptually simpler and computationally much less demanding than the discrete-fracture approach, and is able to handle fracture-matrix interaction more easily than the discrete-fracture model. For these reasons, the dual-continuum approach has been used as the main approach for modeling fluid flow, heat transfer, and chemical transport through fractured reservoirs (Wu et al. 1999; Wu et al. 2007).

Multi-continuum approaches, as discussed in this paper, include the classical double-porosity model (Warren and Root, 1963), the dual-permeability concept, and the more rigorous dual-continuum generalization of the MINC (Pruess and Narasimhan, 1985) and the multi-continuum model (Wu and Pruess, 1988) for modeling flow in fractured porous media. In the double-porosity model, a flow domain is composed of matrix blocks with low permeability, embedded in a network of interconnected fractures. Global flow and transport in the formation occur only through the fracture system, conceptualized as an effective continuum, and matrix blocks are treated as spatially distributed sinks or sources to the fracture system without accounting for global matrix-matrix flow. In comparison, the MINC concept (Pruess and Narasimhan, 1985) is able to describe gradients of pressures, temperatures, or concentrations near matrix surface and inside the matrix—by further subdividing individual matrix blocks with one- or multidimensional strings of nested meshes. Therefore, the MINC model in general provides a better numerical approximation for transient fracture-matrix interactions than the double-porosity model, and may be suitable for describing transient gas flow in tight fractured reservoir.

In this work, we present a generalized mathematical model for simulating multiphase flow of tight gas in porous/fractured reservoirs using the general, multi-continuum modeling approach. The model incorporates the following processes: (1) Klinkenberg effect, (2) non-Newtonian behavior (i.e., threshold pressure gradient for flow to occur); (3) non-Darcy flow with inertial effects; and (4) rock deformation due to changes in the stress field. In particular, we separate the effect of rock mechanical deformation from molecular interaction between fluids and rock materials. The former effect is included using intrinsic permeability and porosity relationships, while the latter is accounted for by an apparent viscosity for non-Newtonian, non-Darcy behavior or a modified permeability for Klinkrnberg effect.

The proposed mathematical model has been implemented into a multiphase, multidimensional reservoir simulator. In the numerical model, specifically, a control-volume, integral finite-difference method is used for spatial discretization with an unstructured grid, and a first-order finite-difference scheme is adapted for temporal discretization. The resulting discrete nonlinear equations are solved fully implicitly by Newton iteration.

Mathematical Model

Let us consider a multiphase, isothermal system consisting of two fluid phases or two mass components, gas and liquid (brine). In an isothermal system containing the two mass components, two mass-balance equations are needed to describe two-phase flow in porous or fractured media (note that solution gas in the liquid phase is considered to be small and is ignored). For flow of phase β (as a subscript, β =g for gas and = w for water), mass conservation to each phase or component leads to

$$\frac{\partial}{\partial t}\left(\phi S_\beta \rho_\beta\right) = -\nabla \bullet \left(\rho_\beta \mathbf{v}_\beta\right) + q_\beta \tag{1}$$

where ϕ is the effective porosity of the medium, treated as a function of the effective stress; S_β is the saturation of phase β; ρ_β is the density of phase β under reservoir conditions; q_β is the sink/source term of phase (component) β per unit volume of formation; and $\mathbf{v}_\beta$ is the flow velocity (or volumetric flow rate), defined differently under different flow regimes or situations, as discussed in the following.

Darcy's Flow: When the Darcy's law is applicable, the velocity, $\mathbf{v}_\beta$, is defined as:

$$\mathbf{v}_\beta = -\frac{k k_{r\beta}}{\mu_\beta}\left(\nabla \Phi_\beta\right) \tag{2}$$

where k is the absolute/intrinsic permeability of the formation, treated as a function of effective stress for stress sensitive reservoirs or pressure with Klinkenberg effect; $k_{r\beta}$ is relative permeability to phase β, treated as a function of fluid saturation; μ_β is the viscosity of phase β as a function of pressure; and $\nabla \Phi_\beta$ is flow potential gradient,, defined as,

$$\nabla \Phi_\beta = \left(\nabla P_\beta - \rho_\beta g \nabla D\right) \tag{3}$$

where P_β is the pressure of phase β; g is gravitational acceleration; and D is the depth from a datum.

Non-Darcy's Flow: In addition to multiphase Darcy flow, non-Darcy flow may also occur between and among the continua in tight gas reservoirs. The flow velocity, $\mathbf{v}_\beta$, (or volumetric flow rate) for non-Darcy flow of each fluid may be described using the multiphase extension of the *Forchheimer* equation (e.g., Wu, 2002):

$$-\left(\nabla \Phi_\beta\right) = \frac{\mu_\beta}{k_{r\beta}} k\, \mathbf{v}_\beta + \beta_\beta \rho_\beta \mathbf{v}_\beta \left|\mathbf{v}_\beta\right| \tag{4}$$

where β_β is the effective non-Darcy flow coefficient with a unit m^{-1} for fluid β under multiphase flow conditions.

Non-Newtonian Flow: Non-Newtonian flow is used in this work to describe conditions where flow may not occur until the pressure or potential gradient reaches a certain threshold value, which is similar to Bingham non-Newtonian fluid flow in porous media. Such a threshold-pressure-gradient concept is commonly used to describe nonlinear flow behavior in low permeability reservoirs (Xiong et al. 2008). Instead of introducing an apparent viscosity for Bingham fluid, an effective potential gradient approach, as follows, has been proven to be more efficient numerically (Wu et al., 1992). Using the effective potential gradient, as illustrated by Figure 1, the flow of gas or liquid in a low-permeability reservoir is described by

$$\mathbf{v}_\beta = -\frac{k k_{r\beta}}{\mu_\beta}\left(\nabla\Phi_e^\beta\right) \tag{5}$$

where $\mu_{b,\beta}$ is the Bingham plastic viscosity coefficient for phase β; and $\nabla\Phi_e^\beta$ is the effective potential gradient whose scalar component in the x direction (the flow direction) is defined as (Figure 1),

$$\left(\nabla\Phi_e\right)_x = \left(\nabla\Phi\right)_x - G \quad \text{for} \quad \left(\nabla\Phi\right)_x > G \tag{6a}$$

$$\left(\nabla\Phi_e\right)_x = \left(\nabla\Phi\right)_x + G \quad \text{for} \quad \left(\nabla\Phi\right)_x < -G \tag{6b}$$

$$\left(\nabla\Phi_e\right)_x = 0 \quad \text{for} \quad -G < \left(\nabla\Phi\right)_x < G \tag{6c}$$

where G is the threshold (or minimum) potential gradient for the fluid to become mobile.

Stress-Sensitive Formation: Based on the observation from experimental results (e.g., Xiong et at. 2008; Wu et al. 2008) and previous research (Terzaghi, 1943; Rutqvist et al. 2002), the effective porosity, permeability, and capillary pressure of rock are assumed to correlate with the mean effective stress (σ'_m) as:

$$\sigma'_m = \sigma_m(x, y, z, P) - \alpha P \tag{7}$$

where σ_m is mean total stress; α is Biot's effective parameter (Biot, 1941), and P is wetting-phase or average pressure. The mean total stress can be treated as constant but, in general, it is estimated by the equation

$$\sigma_m(x,y,z,P) = (\sigma_x(x,y,z,P) + \sigma_y(x,y,z,P) + \sigma_z(x,y,z,P))/3 \tag{8}$$

where σ_x, σ_y, and σ_z are total stress in x, y, and z- directions, respectively.

With the definition of the mean effective stress in Equation (8), the effective porosity of formation is defined as a function of mean effective stress only,

$$\phi = \phi\left(\sigma'_m\right) \tag{9}$$

Similarly, the intrinsic permeability is related to the effective stress, i.e.,

$$k = k\left(\sigma'_m\right) \tag{10}$$

For capillary-pressure functions, the impact of rock-deformation or pore-change is accounted for using the Leverett function (Leverett, 1941),

$$P_c = C_p P_c^0\left(S_w\right)\frac{\sqrt{k^0/\phi^0}}{\sqrt{k(\sigma'_m)/\phi(\sigma'_m)}} \tag{11}$$

where P_c is the capillary pressure between gas and water as a function of water or gas saturation; C_p is a constant; and the superscript 0 denotes reference or zero-stress condition.

To incorporate rock-deformation effects at a given site, the proposed model correlations, Equations (9), (10), and (11), need to be determined from laboratory or field studies. The key for applicability of these models in multiphase flow simulations coupled with rock deformation is that the distribution of effective stress or total stress field must be predetermined as a function of spatial coordinates and pressure fields, as in Equations (7) and (8). In practice, the stress distribution may be estimated analytically, numerically, or from field measurements, because changes in effective stress are primarily caused by changes in reservoir pressure. These models can be significantly simplified for coupling multiphase gas flow with rock deformation in stress-sensitive formations in numerical simulation, if the *in situ* total stress in reservoirs is constant or a function of spatial coordinates as well as fluid pressure.

Klinkenberg Effect: In low-permeability formation or under low pressure condition, the Klinkenberg effect may be too significant to be ignored when modeling gas flow in reservoirs (Wu et al. 1998). Under such flow conditions, absolute permeability for the gas phase is written as a function of gas pressure as,

$$k_g = k_\infty\left(1 + \frac{b}{P_g}\right) \tag{12}$$

where k_∞ is constant, absolute gas-phase permeability under very large gas-phase pressure (where the Klinkenberg effect is minimized); and b is the Klinkenberg factor, depending on the pore structure of the medium and formation temperature.

Constitutive Relations: The governing equation—Equation (1)—of mass conservation for two-phase flow needs to be supplemented with constitutive equations, which express all the parameters as functions of a set of primary thermodynamic variables. The following relationships will be used to complete the description of multiple-phase flow, coupling with Darcy or non-Darcy flow, non-Newtonian flow, Klinkenberg effects, or rock deformation in stress-sensitive porous media. In addition to the two governing equations of (1), there is a supplementary equation,

$$S_w + S_g = 1 \tag{13}$$

with relative permeability and capillary functions. The relative permeabilities are assumed to be functions of fluid saturations only, such that they are unaffected by other nonlinear behavior or rock deformation. The relative permeability to the two phases may be described (Aziz and Settari, 1979),

$$k_{r\beta} = k_{r\beta}(S_w) \tag{14}$$

Capillary pressure is needed to relate pressures between the gas and liquid phases and is treated as a function of water saturation. For stress sensitive rock, the capillary function is modified using the Leverett function of equation (11). At reference or zero stress condition, the capillary pressure between the gas and water phases is defined as:

$$P_c^0 = P_g - P_w = P_c(S_w) \tag{15}$$

Numerical Formulation

The system of equations, as discussed above, for multiphase flow of gas and water, coupled with non-Darcy, non-Newtonian, Klinkenberg, or rock deformation, is highly nonlinear, and in general needs to be solved numerically. The methodology for using numerical approaches to simulate the multiphase flow consists of the following three steps: (1) spatial discretization of mass conservation equations, (2) time discretization; and (3) iterative approaches to solve the resulting nonlinear, discrete algebraic equations. A mass-conserving discretization scheme, based on finite or integral finite-difference or finite-element methods, is used and discussed here.

The mass-balance Equation (1) is discretized in space using a control-volume or integral finite difference concept (Pruess et al. 1999). The control-volume approach provides a general spatial discretization scheme that can represent a one-, two- or three-dimensional domain using a set of discrete meshes. Time discretization is carried out using a backward, first-order, fully implicit finite-difference scheme. Specifically, the multiphase flow equations, as discussed in the section above, have been implemented into a three-phase reservoir simulator (Wu, 2000). As implemented numerically, Equation (1) is discretized in space using an integral finite-difference or control-volume scheme for a porous and/or fractured medium with an unstructured grid. The time discretization is carried out with a backward, first-order, finite-difference scheme. The discrete nonlinear equations for gas and water flow at node i are as follows (for β = g and w):

$$\left\{\left(\phi\, S_\beta \rho_\beta\right)_i^{n+1} - \left(\phi\, S_\beta \rho_\beta\right)_i^{n}\right\}\frac{V_i}{\Delta t} = \sum_{j\in\eta_i} \mathrm{flow}_{\beta,ij}^{n+1} + Q_{\beta i}^{n+1} \tag{16}$$

where the superscript n denotes the previous time level; n+1 is the current time level; V_i is the volume of element i (porous or fractured block); Δt is time step size; η_i contains the set of neighboring elements (j) (porous or fractured) to which element i is directly connected; $\mathrm{flow}_{\beta,ij}^{n+1}$ is the mass "flow" term for phase β between elements i and j; and $Q_{\beta i}$ is the mass sink/source term at element i, for phase β.

The "flow" term ($\mathrm{flow}_{\beta,ij}^{n+1}$) in Equation (16) for multiphase flow is evaluated differently for different flow conditions. Under the condition of Darcy flow, which may be subject to Klinkenberg or rock deformation effects, the flow term is described by a discrete version of Darcy's flow, i.e., the mass flux of fluid phase β along the connection is given by:

$$\mathrm{flow}_{\beta,ij} = \lambda_{\beta,ij+1/2}\gamma_{ij}\left(\Phi_{\beta j} - \Phi_{\beta i}\right) \tag{17}$$

where $\lambda_{\beta,i\,j+1/2}$ is the mobility term corresponding to phase β, defined as:

$$\lambda_{\beta,i\,j+1/2} = \left(\frac{\rho_\beta k_{r\beta}}{\mu_\beta}\right)_{ij+1/2} \tag{18}$$

The subscript ij+1/2 denotes a proper averaging or weighting of properties at the interface between the two elements i and j, discussed below; and γ_{ij} is the transmissivity, defined differently for finite-difference or finite-element discretization. If the integral finite-difference scheme (Pruess et al. 1999) is used, the transmissivity is calculated as:

$$\gamma_{ij} = \frac{A_{ij} k_{i\,j+1/2}}{d_i + d_j} \tag{19}$$

where A_{ij} is the common interface area between the connected blocks or nodes i and j; d_i is the distance from the center of block i to the common interface of blocks i and j; and $k_{ij+1/2}$ is an averaged (such as harmonic-weighted) absolute permeability along the connection between elements i and j. The flow potential term in Equation (17) is defined as

$$\Phi_{\beta i} = P_{\beta i} - \rho_{\beta,ij+1/2}\, g\, D_i \tag{20}$$

Handling Klinkenberg effects: To include the Klinkenberg effect on gas flow, the absolute permeability to gas phase in (19) should be evaluated using Equation (12), as a function of gas phase pressure.

Handling rock deformation effects: If the stress field is predetermined as a function of spatial coordinates and fluid pressure, the effect of rock deformation on fluid flow can be evaluated using (9) for porosity, (10) for absolute permeability, and (11) for capillary pressure, respectively, as functions of effective stress and other primary and secondary variables in numerical formulation.

Handling non-Newtonian flow: In the case that gas or water flow is subject to a threshold potential gradient, the discrete potential gradient in (17) should be replaced by the effective potential gradient, Equation (6) for flow term evaluation.

Handling non-Darcy flow: Under the non-Darcy flow condition of Equation (4), the flow term ($\mathrm{flow}_{\beta,ij}^{n+1}$) in Equation (16) along the connection (i, j), between elements i and j, is numerically defined as (Wu, 2002),

$$\mathrm{flow}_{\beta,ij} = \frac{A_{ij}}{2\left(k\beta_\beta\right)_{ij+1/2}}\left\{-\frac{1}{\lambda_\beta} + \left[\left(\frac{1}{\lambda_\beta}\right)^2 - \bar{\gamma}_{ij}\left(\Phi_{\beta j} - \Phi_{\beta i}\right)\right]^{1/2}\right\} \tag{21}$$

in which the non-Darcy flow transmissivity is defined as,

$$\bar{\gamma}_{ij} = \frac{4\left(k^2 \rho_\beta \beta_\beta\right)_{ij+1/2}}{d_i + d_j} \tag{22}$$

Note that Equation (16), a discrete equation of mass conservation, has the same form regardless of the dimensionality of the model domain, i.e., it applies to one-, two-, or three-dimensional analyses of flow through porous or fractured media.

Numerical Solution Scheme

There are a number of numerical solution techniques that have been developed over the past few decades to solve the nonlinear, discrete equations of reservoir simulations. When handling multiphase flow in a multiphase flow system, the most robust (and highly advisable) approach involves the use a fully implicit scheme. This scheme has the advantage of being able to handle extremely highly nonlinear- problems that often confound methods that involve lower levels of implicitness. In this section, we discuss a general procedure to solve the discrete, nonlinear Equation (16) fully implicitly, using a Newton iteration method.

Let us write the discrete nonlinear Equation (16) in a residual form as

$$R_{\beta i} = \left\{\left(\phi\, S_\beta \rho_\beta\right)_i^{n+1} - \left(\phi\, S_\beta \rho_\beta\right)_i^{n}\right\}\frac{V_i}{\Delta t} - \sum_{j\in\eta_i} \mathrm{flow}_{\beta,ij}^{n+1} - Q_{\beta i}^{n+1} \tag{22}$$

(i = 1, 2, 3, …, N) and (for β = g and w)

where N is the total number of nodes of the grid. Equation (22) defines a set of (2 × N) coupled nonlinear mass balance equations that need to be solved simultaneously. In general, two primary variables per node are needed to use the Newton iteration for the associated 2 equations per node. The primary variables selected are the pressure of one of the fluid phases and saturation. The rest of the dependent variables, such as relative permeability, capillary pressures, viscosity, and densities, as well as nonselected pressure and saturation, are treated as secondary variables, which are calculated from the primary variables.

In terms of the primary variables, the residual equation, Equation (22), at a node i is regarded as a function of the primary variables at not only node I, but also at all its directly neighboring nodes j. The Newton iteration scheme gives rise to

$$\sum_m \frac{\partial R_i^{k,n+1}\left(x_{m,p}\right)}{\partial x_m}\left(\delta x_{m,p+1}\right) = -R_i^{k,n+1}\left(x_{m,p}\right) \tag{23}$$

where x_m is the primary variable m with m = 1 and 2, respectively, at node i and all its direct neighbors; p is the iteration level; and i =1, 2, 3, …, N. The primary variables in Equation (23) need to be updated after each iteration:

$$x_{m,p+1} = x_{m,p} + \delta x_{m,p+1} \tag{24}$$

The Newton iteration process continues until the residuals, $R_n^{k,n+1}$, or changes in the primary variables $\delta x_{m,p+1}$ over an

iteration are reduced below preset convergence tolerances. In addition, the numerical method is used to construct the Jacobian matrix for Equation (23), as outlined in Forsyth et al. (1995). At each Newton iteration, Equation (23), represents a system of $2 \times N$ linearized algebraic equations with sparse matrices, which are solved by a linear equation solver.

Treatment of Initial and Boundary Conditions

A set of initial conditions is required to start a transient simulation, i.e., a complete set of primary variables need to be specified for every gridblock or node. A commonly used procedure for specifying initial conditions is equilibrium calculation or restart option, in which a complete set of initial conditions or primary unknowns is generated in a previous simulation, with proper boundary conditions described.

Dirichlet boundary conditions are handled with the "inactive cell" or "big-volume" method, as normally used in the TOUGH2 code (Pruess et al. 1999). In this method, a constant pressure/saturation node is specified as an inactive cell or with a huge volume, while keeping all the other geometric properties of the mesh unchanged. For flux or Neuman boundary conditions, and multilayered wells, a general procedure for handling such boundary conditions is discussed in Wu et al. (1996 and 2000).

Handling Fractured Media

The technique used in this work for handling multiphase flow through fractured rock follows a generalized dual-continuum methodology (Pruess and Narasimhan, 1985; Wu and Pruess, 1988; Pruess et al. 1999). This method describes fracture and matrix flow and interactions using a multicontinuum numerical approach, including the double- or multi-porosity method, the dual-permeability method, and the more general MINC method. The multiphase flow formulation, Equations (2), (4), and (5), or their discrete forms, Equations (17) and (21), are applicable to both single-continuum and multicontinuum media. Using the dual-continuum concept, the flow equations can be used to describe multiphase flow both in fractures and within the matrix blocks, as well as the fracture-matrix interaction. However, special attention needs to be paid to treating fracture-matrix flow. In this case, the flow between fractures and the matrix is still evaluated using Equation (17), i.e., such flow is assumed to obey Darcy's law. Then the transmissivity of the fracture-matrix flow system (when the double-porosity model is employed) is given by

$$\gamma_{ij} = \frac{A_{FM} k_M}{l_{FM}} \tag{25}$$

where A_{FM} is the total interfacial area between fractures and the matrix of elements i and j (of which, one of them is a fracture and the other a matrix block); k_M is the matrix absolute permeability along the fracture-matrix connection; and l_{FM} is a characteristic distance for flow crossing fracture-matrix interfaces, which can be determined for idealized 1-D, 2-D and 3-D dimensional rectangular matrix blocks using the double-porosity model (e.g., Warren and Root, 1963; Wu and Pruess, 1988).

Small-fracture concept: As can be observed in most fractured formations, there are more small-scale fractures than large ones. To capture effects of small-scale fractures in tight gas reservoirs, we conceptualize the fracture-matrix system as consisting of a single porous-medium rock matrix and two types of fractures: (1) "large" *globally connected* fractures and (2) "small" fractures that are *locally connected* to the large fractures and the rock matrix (Wu et al. 2004). Figure 2 illustrates this triple-continuum concept, as compared to ECM, double-porosity, and dual-permeability concepts. The triple-continuum method (Figure 2d) extends the dual-permeability concept by adding one more connection (via small fractures) between the large fractures and the matrix blocks. Note that fractures not directly connected with large fractures (i.e., fractures that are isolated within the matrix) are not considered part of the small fracture continuum in this model. Instead, these fractures are considered as part of the matrix continuum. This triple continuum concept may be particularly suitable for modeling gas flow through tight fractured or shale reservoirs, because field data often show that there is a large number of small- or micro-fractures, which do not contribute to global flow, but provide large connecting areas for interaction between large fractures and matrix systems. In addition, small fractures also provide a larger storage space than large fractures in general.

Figure 3 illustrates the triple-continuum conceptualization for a fracture-matrix system in which the small-fracture/matrix connections occur in only one dimension. A second set of small-fracture/matrix connections can also be added to occur in two dimensions (i.e., horizontally and vertically, Figure 4). In a similar manner, a third set of fractures can be added to extend the system of small-fracture/matrix interactions in three dimensions. Note that the triple-continuum model is not limited to the orthogonal idealization of the fracture network systems, as illustrated in Figures 3 and 4. Irregular and stochastic distributions of small and large fractures can be handled using a similar approach to the MINC methodology (Pruess, 1983), as long as the actual distribution patterns are known. In principle, the proposed triple-continuum model, like the dual-continuum approach, uses an "effective" porous medium to approximate the two types of fractures as well as the rock matrix, and considers the three continua to be spatially overlapped. Like other continuum approaches, the triple-continuum model relies on the assumption that approximate thermodynamic equilibrium exists (locally) within each of the three continua at all times at a given location. Based on the local equilibrium assumption, we can define thermodynamic variables, such as pressures and saturations, for each continuum. In the triple-continuum approach, processes of flow and transport in fractured rocks are described separately, using a triplet of governing equations for the two fracture and matrix

continua. This conceptualization results in a set of partial differential equations for flow in each continuum, which are in the same form as that for a single porous medium, such as Equation (1).

To evaluate flow terms between small fractures and large fractures or between small fractures and the matrix, we require additional geometric parameters such as the interface areas and characteristic lengths along these connections. In the demonstration examples of this study, small fractures are represented by one cell interacting locally with large fracture and matrix systems (Figure 2). In this case, Table 1 summarizes the parameters of the equations used to determine the characteristic distances for calculating flow between the three continua for regular one-, two- and three-dimensional large fracture networks, each with uniform distributions of small fractures. The quasi-steady-state flow assumption of Warren and Root (1963) is used to derive the characteristic distances, as listed in Table 1, when the matrix is represented by only one gridblock. The flow distance between small fractures (f) and large fractures (F) is taken to be half the characteristic length of the small fractures within a matrix block (Figures 3 and 4). Furthermore, the interface areas between small fractures and matrix (M) are calculated using the geometric data of the small fractures. Interface areas between large fractures and the matrix and between large fractures and small fractures are estimated using the geometry of the large fractures. This treatment has implicitly defined the permeabilities of the two fractures in a continuum sense, such that bulk connection areas are needed to calculate Darcy flow between the two fracture continua. In summary, we extend the Warren and Root (1963) approach to evaluate interactions along F-M and f-M connections in our triple-continuum model.

Within the context of the dual-continuum concept, the proposed approach can be applied to different matrix discretizations, such as double-porosity, dual-permeability, or MINC grids. When describing flow through triple-continuum fractured rock, one of the main challenges is to generate a mesh that represents both types of fractures as well as the matrix continuum. This triple-continuum, fracture-matrix mesh can be generated using the MINC concept (Pruess, 1983), i.e., starting from a primary or single-porous medium mesh that uses bulk volume of formation and layering only. Then, we use geometric information (e.g., fracture density, aperture, lengths, and orientations) of the corresponding two-type fractures within the basic formation subdomains (i.e., a single gridblock of the primary mesh), large fractures are lumped into the large fracture continuum and small fractures form the small fracture continuum, respectively. The remaining part of the basic subdomain is regarded as the matrix continuum.

Once a proper grid of a fracture-matrix system is generated, fracture and matrix blocks are identified to represent fracture and matrix domains, separately. Formally they are treated identically for the solution in the model simulation. However, physically consistent fracture and matrix properties, parameter weighting schemes, and modeling conditions must be appropriately specified for both fracture and matrix systems. The mathematical and numerical formulations discussed above are applicable to both single-continuum and multicontinuum media using the generalized multicontinuum concept, as long as the physical processes concerned can be described in a continuum sense within either continuum. Figures 3 and 4 show two typical conceptual models, or triple-continuum approximation, for modeling fracture-matrix flow in fractured reservoirs with two-scaled fractures. All these cases and scenarios could all be considered to be special cases of the model formulation we discuss above.

Application Examples

To demonstrate the usefulness of the proposed generalized multi-continuum modeling approach in modeling gas flow through tight or fractured gas reservoirs, we present three application examples: (1) transient gas flow in a porous medium (or single-porosity medium); (2) transient gas flow in a double-porosity medium, and (3) transient gas flow in a triple-continuum medium with two-scaled (large and small) fractures. In these examples, we are concerned with transient gas flow towards a well that fully penetrates a radially infinite, horizontal, and uniformly porous or fractured reservoir. The reservoir formation is at liquid-gas, two-phase condition, however, the liquid saturation is set at residual values as an immobile phase. This is a single-phase gas flow problem and is modeled by the two phase flow reservoir simulator. The immobile liquid flow is controlled by liquid relative permeability curves.

In numerical discretization, a radial reservoir (r_e = 100,000 m) of 1 m thick is represented by a 1-D (primary) radial grid of 1,102 radial increments of size Δr that increases logarithmically from the well radius, r_w = 0.1 m. For both double-porosity and triple-porosity models, the 1-D primary radial grid is used as the basis to generate the double-porosity and triple-porosity grids, in which the (large-) fracture-matrix system consists of one horizontal large-fracture plate (fracture spacing A = 1.0) and uniform disk-shaped matrix blocks. Note that in our testing problems for analyzing and comparing model results, the double-porosity model consists of only the large fracture and matrix system, while the triple-continuum model also includes the small fractures. The large fractures and matrix in the double-porosity model have the same properties as those in the triple-continuum model. In the triple-continuum conceptual model, (similar to that shown in Figure 3, but with the large fracture being horizontal), small fractures are uniformly distributed and perpendicular to large horizontal fractures.

Fractures and matrix parameters used for the examples are given in Table 2. Note that the single-porosity example uses the same properties as those for the matrix of fractured rock in Table 2. Figure 5 shows the relationship between gas viscosity and pressure. Figure 6 gives the correlation of gas formation volume factor and gas pressure, treated as a real gas. The functional relations for gas viscosity and formation volume factor (or density), as shown in Figures 5 and 6, are used in the three simulation examples. In simulations, liquid is treated as immobile for both matrix and fracture systems, and the only flowing phase is the gas phase.

Figure 7 shows the results for transient gas flow in the single-porosity medium with permeability of 10 μD and gas production rate of 100 standard cubic meters per day. Figure 7 presents a comparison of simulated gas pressures at the well with the Klinkenberg effect ($b = 3.6\times10^6$ Pa) and without Klinkenberg effect during the one year production. The figure indicates some difference made by the Klinkenberg effect under the low-permeability reservoirs.

Figure 8 shows the results and comparisons for Problems #2 (double-porosity) and #3 (triple-continuum). In these two scenarios, the gas production rates are at 1,000 standard cubic meters per days and the Klinkenberg effect is not included in the plots, because of the higher fracture permeability and the insignificant effect. In the simulations, we included the Klinkeberg effects. The comparison of the two model results on Figure 8 indicates that the triple-continuum model, with small fractures providing both storage space and transitional mobility from matrix to large fractures, predicts a smaller pressure drop for the same production rate because of contributions of small fractures, as compared to the double-porosity model for the first 0.1 day. Eventually, the two models exhibit almost the same pressure changes, because the gas produced is from matrix systems with the same matrix properties in both models. The small difference in pressure variations at well is due also to the small porosity (0.005) in this case (Table 2) for small fractures. In comparison, Figure 9 shows the comparison with a larger small-fracture porosity (0.05) and the larger small fracture pore space results in small pressure drops throughout the one-year production with the triple-continuum model. Note that the differences in pressure responses at wells between the double-porosity and triple-continuum models may be small in the sample problems, our main purpose of proposing the small-fracture or multiple-scaled fracture model is actually for enhancing gas recovery rates from low-permeability reservoirs by improving overall fracture-matrix interacting areas and transmissivity between low-permeability matrix and production wells, which could be achieved by formation stimulation technology.

Summary

In this paper, we present a generalized mathematical model for gas flow in two-phase systems of porous or fractured tight-gas reservoirs. To describe gas flow behavior in such low-permeability, highly heterogeneous porous or fractured, and stress-sensitive rock, the model formulation incorporates many relevant physical processes, i.e., Klinkenberg effect, non-Newtonian behavior, non-Darcy flow with inertial effect, and coupled rock deformation and fluid flow. The proposed mathematical model has been implemented and tested using a multiphase, multidimensional reservoir simulator. The numerical implementation of the unified formulation is based on a control-volume spatial discretization, using an unstructured grid, and the time discretized with a fully implicit finite-difference method. The final discrete linear or nonlinear equations are handled fully implicitly, using Newton iteration.

The proposed numerical modeling approach, based on a general multiple-continuum concept, is suitable for modeling various types of fractured reservoirs, including double-, triple-, and other multiple-continuum conceptual models for multi-scaled fractures and matrix systems. The proposed general modeling methodology is demonstrated for its application in the example cases where transient gas flow occurs through single-porosity, double-porosity, and triple-continuum media. The model application to actual tight gas reservoirs is an on-going research project and will be reported in the future.

Acknowledgments

This work was supported in part by Colorado School of Mines and by National Basic Research Program of China (973 Program), “Studying the Fundamentals of the Carbonate Karst Reservoir Development 2006CB202400.” The authors would like to thank Jennifer Miskimins and Matthew Reagan for reviewing this manuscript.

Nomenclature

a	small-fracture spacing along large fracture or the x-direction (m)
A	large-fracture spacing along large fracture or the x-direction (m)
A_{Ff}	total combined area of large fracture and small fracture connections per unit volume of rock (m^2/m^3)
A_{FM}	total combined area of large fracture and matrix connections per unit volume of rock (m^2/m^3)
A_{ij}	interface areas between two gridblock i and j (m^2)
b	Klinkenberg factor (Pa)
b	small-fracture spacing along large-fracture or the y-direction (m)
B	large-fracture spacing along large-fracture or the y-direction (m)
c	small-fracture spacing along large fracture or the z-direction (m)
C	large-fracture spacing along large fracture or the z-direction (m)
C_f	total compressibility in small-fracture continuum (Pa^{-1})
C_F	total compressibility in large-fracture continuum (Pa^{-1})
C_M	total compressibility in matrix continuum (Pa^{-1})
$\text{flow}_{\beta,ij}^{n+1}$	mass flow components of fluid β ($kg/s/m^2$) along connection ij of time level n+1
g	gravitation constant (m/s^2)
G	threshold pressure or potential gradient (Pa/m)
h	thickness of formation (m)

k	absolute permeability of porous media (m^2)
k_F	absolute permeability of large fracture continuum (m^2)
k_f	absolute permeability of small fracture continuum (m^2)
k_M	absolute permeability of matrix continuum (m^2)
$k_{r\beta}$	relative permeability to phase β
k_∞	absolute permeability at large gas pressure
l_f, l_F	characteristic length (m) of small and large fractures in the x-direction and y-direction, respectively
l_{Ff}, l_{FM}, l_{fM}	characteristic distance (m) between F-f, F-M, and f- M, respectively, (defined in Table (1)
l_x, l_y, l_z	half-length (m) of small fractures, respectively, (defined in Table 1, illustrated in Figures 3 and 4)
P	Pressure (Pa)
P_β	pressure of phase β (Pa)
P_c	capillary pressure (Pa)
q_β	source/sink - or fracture matrix interaction of mass for phase β (kg/s m^3)
Q_β^{n+1}	source/sink or fracture-matrix exchange terms for phase β (kg/s) of time level n+1
R_β	residual term of mass balance of phase β (kg/m^3) of time level n+1
r_w	well radius (m)
S_β	fluid saturation of phase β
t	time (s)
Δt	time step (s)
V_i	volume of gridblock i (m^3)
$\mathbf{v}_\beta$	Darcy's or volumetric velocity of phase β (m/s)

Greek Symbols

α	Biot's effective parameter
β_β	effective non-Darcy flow coefficient for phase β (m^{-1}) of
ϕ	effective porosity of formation
ϕ_f	effective porosity of a small fracture continuum
ϕ_F	effective porosity of a large fracture continuum
ϕ_M	effective porosity of a matrix continuum
Φ_β	flow potential (Pa)
γ_{ij}	transmissivity (m^3)
$\bar{\gamma}_{ij}$	transmissivity for non-Darcy flow (m^{-1})
$\lambda_{\beta,ij+1/2}$	mobility of phase β between gridblcoks i and j
λ_{FM}	F-f interporosity parameter (defined in Table 2)
μ_β	viscosity of phase β (Pa•s)
ρ_β	density of phase β at *in situ* conditions (kg/m^3)
σ_m	mean total stress (Pa)
σ'_m	mean effective stress (Pa)

Subscripts

c	capillary
f	denote small fracture
F	denotes large fracture
g	gas
i	gridblock i
j	gridblock j
m	mean
M	denotes matrix
w	water

β	index of fluid phase

Superscripts

0	zero stress condition
k	index for mass components.
n	previous time level n
n+1	current time level n+1
p	iteration level

References

Aziz, k. and A. Settari, *Petroleum Reservoir Simulation*, Applied Science Publishers LTD, London, 1979.

Barenblatt, G. I., I. P. Zheltov and I. N. Kochina, Basic concepts in the theory of seepage of homogeneous liquids in fissured rocks, PMM, *Sov. Appl. Math. Mech*., 24(5), 852-864, 1960.

Bear, J., *Dynamics of Fluids in Porous Media.* American Elsevier Publishing Company, New York, 1972.

Biot, M. A., General Theory of Three Dimensional Consolidation, J. Appl Phys., 12:57-64, 1941.

Forsyth, P. A., Y. S. Wu and K. Pruess, Robust numerical methods for saturated-unsaturated flow with dry initial conditions in heterogeneous media, *Advance in Water Resources*, 18, 25-38, 1955

Kazemi, H., Pressure transient analysis of naturally fractured reservoirs with uniform fracture distribution. *Soc. Pet. Eng.* ., 451-62. *Trans., AIME*, 246, 1969.

Leverett, M. C., Capillary Behavior in Porous Media, *Trans AIME*, 142:341-358, 1941.

Pruess, K., C. Oldenburg and G. Moridis, *TOUGH2 User's Guide, Version 2.0,* Report LBNL-43134, Berkeley, California: Lawrence Berkeley National Laboratory, 1999.

Pruess, K. and T. N. Narasimhan, A practical method for modeling fluid and heat flow in fractured porous media, *Soc. Pet. Eng. J.*, 25, 14-26, 1985.

Pruess, K., GMINC-A *mesh generator for flow simulations in fractured reservoirs*, Report LBL-15227, Berkeley, California: Lawrence Berkeley National Laboratory, 1983.

Rutqvist, J. Y. S. Wu, C. F. Tsang, and G. S. Bodvarsson, A modeling approach for analysis of coupled multiphase fluid flow, heat transfer, and deformation in fractured porous rock, *International Journal of Rock Mechanics and Mining Sciences*, 39:429-442, 2002.

Snow, D. T., A parallel plate model of fractured permeable media, Ph.D. Dissertation, 331. pp., University of California, Berkeley, 1965.

Terzaghi, K., *Theoretical Soil Mechanics*, John Wiley & Sons Inc., New York, 1943.

Warren, J. E., and P. J. Root, The behavior of naturally fractured reservoirs, *Soc. Pet. Eng. J.*, Trans., AIME, 228, 245-255, 1963.

Wu, Y. S., J. Rutqvist, K. Karasaki, Q. Lei, W. Xiong, J. Yuan, M. Liu, and Y. Di, "A mathematic Model for Rock Deformation Effect of Flow in Porous and Fractured Reservoirs," ARMA 08-142, Presented at San Francisco 2008, the 42nd US Rock Mechanics Symposium and 2nd U.S.-Canada Rock Mechanics Symposium, held in San Francisco, June 29-July 2, 2008.

Wu, Y. S., G. Lu, K. Zhang, L. Pan and G. S. Bodvarsson, Analyzing unsaturated flow patterns in fractured rock using an integrated modeling approach, *Hydrogeology Journal*, Vol. 15, 553-572, 2007.

Wu, Y. S., H. H. Liu and G. S. Bodvarsson, A triple-continuum approach for modeling flow and transport processes in fractured rock, *Journal of Contaminant Hydrology*, 73, 145-179, 2004.

Wu, Y. S., "Numerical Simulation of Single-Phase and Multiphase Non-Darcy Flow in Porous and Fractured Reservoirs," *Transport in Porous Media*, Vol. 49, No. 2, pp.209-240, 2002

Wu, Y. S., A virtual node method for handling wellbore boundary conditions in modeling multiphase flow in porous and fractured media, *Water Resources Research*, 36 (3), 807-814, 2000.

Wu, Y. S., On the effective continuum method for modeling multiphase flow, multicomponent transport and heat transfer in fractured rock, "Dynamics of Fluids in Fractured Rocks, Concepts and Recent Advances", Edited by B. Faybishenko, P. A. Witherspoon and S. M. Benson, AGU Geophysical Monograph 122, American Geophysical Union, Washington, DC, 299–312, 2000.

Wu, Y. S., C. Haukwa and G. S. Bodvarsson, A site-scale model for fluid and heat flow in the unsaturated zone of Yucca Mountain, Nevada. *Journal of Contaminant Hydrology*. 38 (1-3), 185-217, 1999.

Wu, Y. S., K. Pruess, and P. Persoff, "Gas Flow in Porous Media with Klinkenberg Effects," *Transport in Porous Media*, Vol.32, pp.117-137, 1998.

Wu, Y. S., P. A. Forsyth and H. Jiang, A consistent approach for applying numerical boundary conditions for subsurface flow, *Journal of Contaminant Hydrology*, Vol. 23, 157-185, 1996.

Wu, Y. S., K. Pruess, and P.A. Witherspoon, "Flow and Displacement of Bingham Non-Newtonian Fluids in Porous Media," *SPE Reservoir Engineering*, pp.369-376, 1992

Wu, Y. S., and K. Pruess, A multiple-porosity method for simulation of naturally fractured petroleum reservoirs, *SPE Reservoir Engineering*, 3, 327-336, 1988.

Xiong, Wei, Qun Lei, Jiangru Yuan, Shusheng Gao, and Yu-Shu Wu, "Behavior of Flow through Low-Permeability Reservoirs," SPE-113144, prepared for presentation at the 2008 SPE EUROPEC Conference to be held in Rome, Italy, 9-12 June 2008

Table 1. Characteristic distances* for evaluating flow terms between two fracture and matrix systems

Large-Fracture Networks	Dimensions of Matrix Blocks	Characteristic Dimension (m) of Large Fractures	Characteristic F-M Distances (m)	Characteristic Dimension (m) of Small Fractures	Characteristic F-f Distances (m)	Characteristic f-M Distances (m)
1-D	A	$l_F = \mathrm{A}$	$l_{FM} = l_F/6$	$l_f = \mathrm{a}$	$l_{Ff} = l_x/2$	$l_{fM} = l_f/6$
2-D	A B	$l_F = \dfrac{2\mathrm{AB}}{\mathrm{A}+\mathrm{B}}$	$l_{FM} = l_F/8$	$l_f = \dfrac{2\mathrm{ab}}{\mathrm{a}+\mathrm{b}}$	$l_{Ff} = \dfrac{l_x + l_y}{2}$	$l_{fM} = l_f/8$
3-D	A B C	$l_F = \dfrac{3\mathrm{ABC}}{\mathrm{AB}+\mathrm{BC}+\mathrm{CA}}$	$l_{FM} = l_F/10$	$l_f = \dfrac{3\mathrm{abc}}{\mathrm{ab}+\mathrm{bc}+\mathrm{ca}}$	$l_{Ff} = \dfrac{l_x + l_y + l_z}{2}$	$l_{fM} = l_f/10$

* Note in Table 1, A, B, and C are dimensions of matrix blocks along x, y, and z directions, respectively. Dimensions a, b, and c are fracture-spacings of small fractures along x, y, and z directions, respectively. Subscript F represents large-fracture, f small-fracture, and M matrix systems, respectively.

Table 2. Parameters used in the three example gas flow problems

Parameter	**Value**	**Unit**
Matrix porosity	$\phi_M = 0.20$	
Large-fracture porosity	$\phi_F = 0.001$	
Small-fracture porosity	$\phi_f = 0.005$	
Large-fracture spacing	A = 1	m
Small-fracture spacing	a = 0.20	m
F characteristic length	$l_x = 0.50$	m
F-f areas per unit volume rock	$A_{Ff} = 20.0$	m^2/m^3
F-M areas per unit volume rock	$A_{Ff} = 2.0$	m^2/m^3
Matrix permeability	$k_M = 1.00\times10^{-17}$	m^2
Large-fracture permeability	$k_F = 1.00\times10^{-15}$	m^2
Small-fracture permeability	$k_f = 1.00\times10^{-16}$	m^2
Gas Production Rate	q = 100 and 1,000	M^3/d
Total compressibility of three media	$C_F=C_M=C_f= 1.0\times10^{-9}$	1/Pa
Well radius	$r_w = 0.1$	m
Formation thickness	h = 1.0	m
Initial formation gas pressure	$P_i = 10^7$	Pa

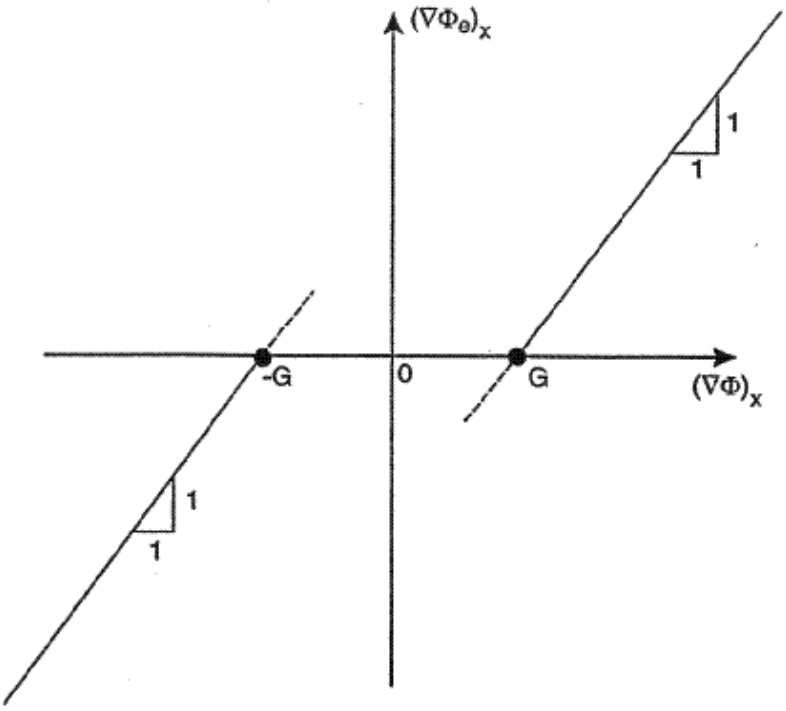

Figure 1. Effective potential gradient for threshold-potential gradient flow, or Bingham non-Newtonian fluid flow (dashed linear extension for numerical calculation of derivatives).

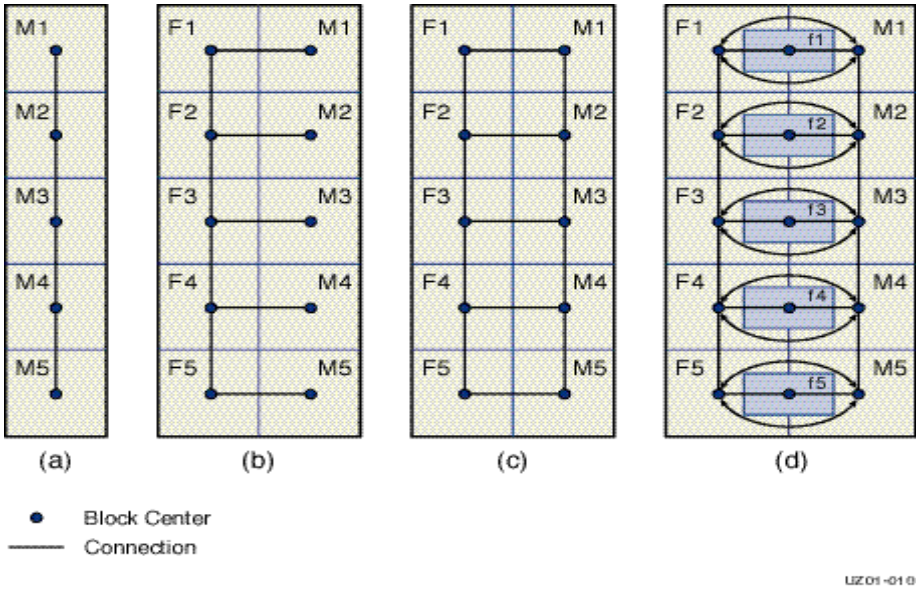

Figure 2. Schematic of different conceptualizations for handling fracture-matrix interactions: (a) effective-continuum model (ECM); (b) double-porosity model; (c) dual-permeability model; and (d) riple-continuum model. (M=matrix; F=large-fractures; f=small-fractures).

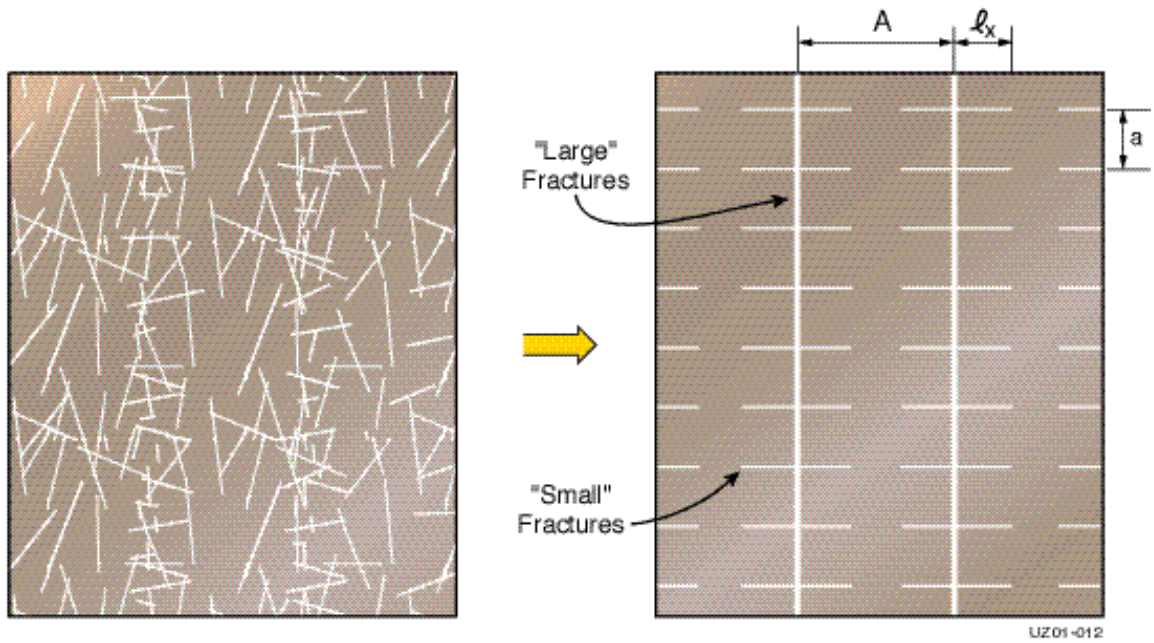

Figure 3. Basic conceptualization for triple-continuum approximation of one-dimensional large-fracture, small-fracture, and rock matrix systems.

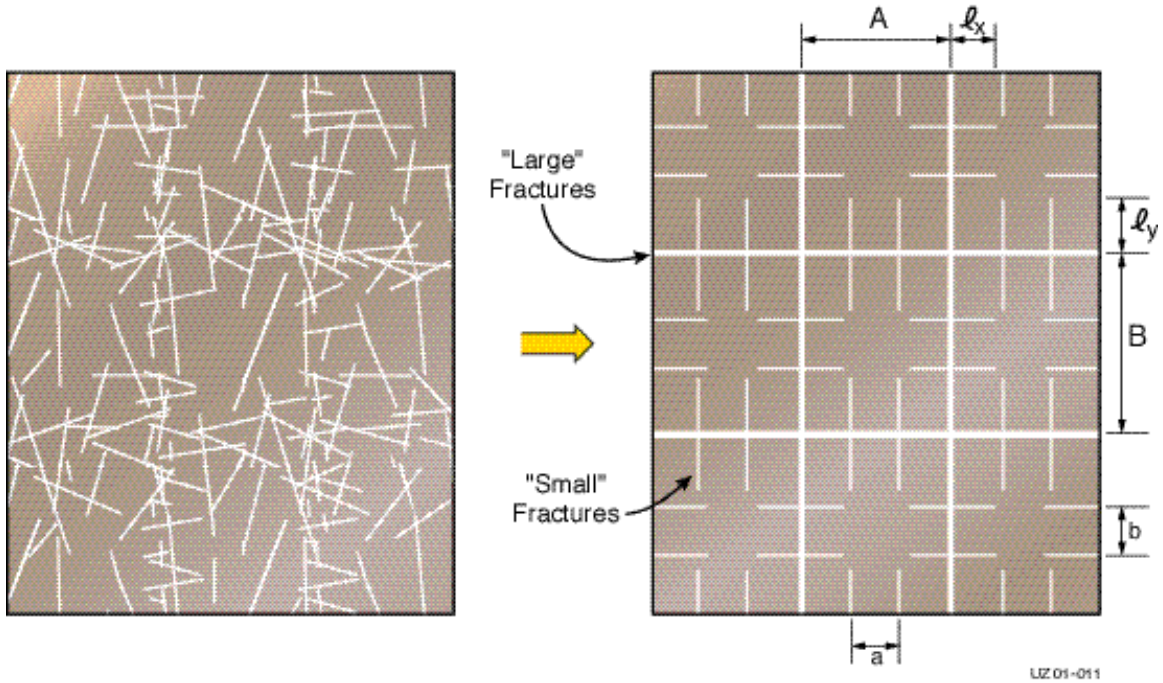

Figure 4. Basic conceptualization for triple-continuum approximation of two-dimensional large-fracture, small-fracture, and rock matrix systems.

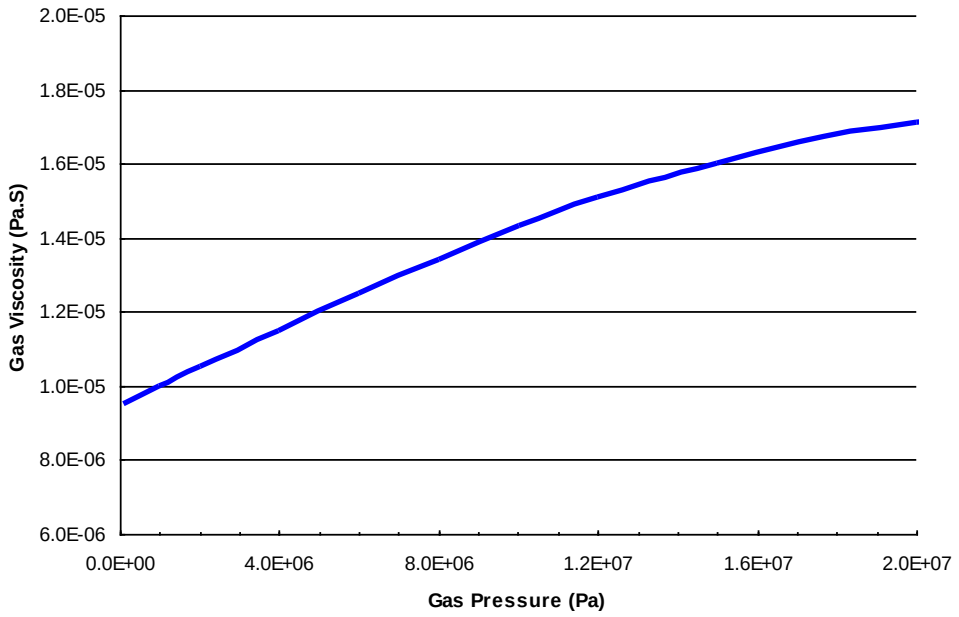

Figure 5. Gas viscosity as a function of gas pressure, used in the three simulation examples.

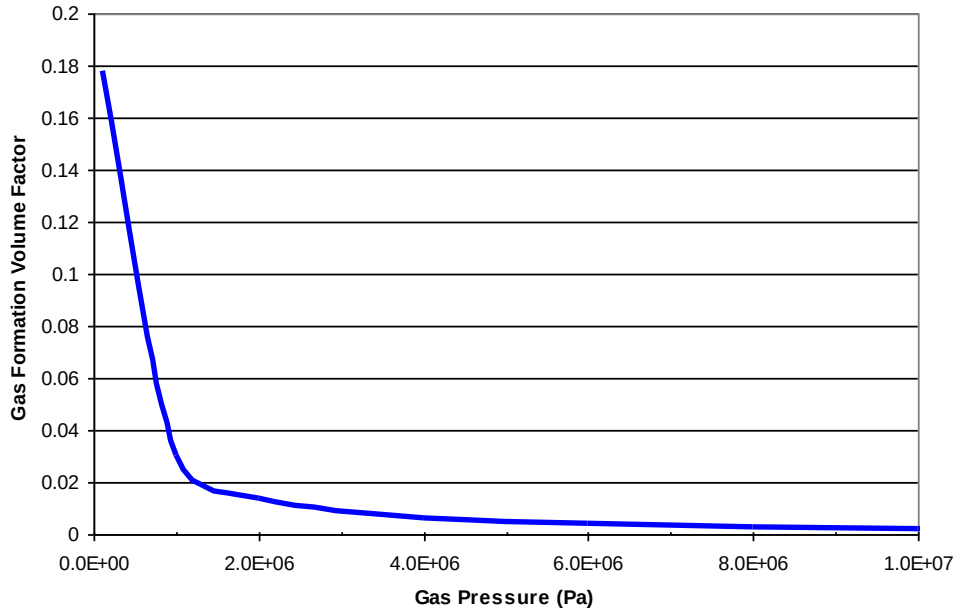

Figure 6. Gas formation volume factor as a function of gas pressure, used in the three simulation examples.

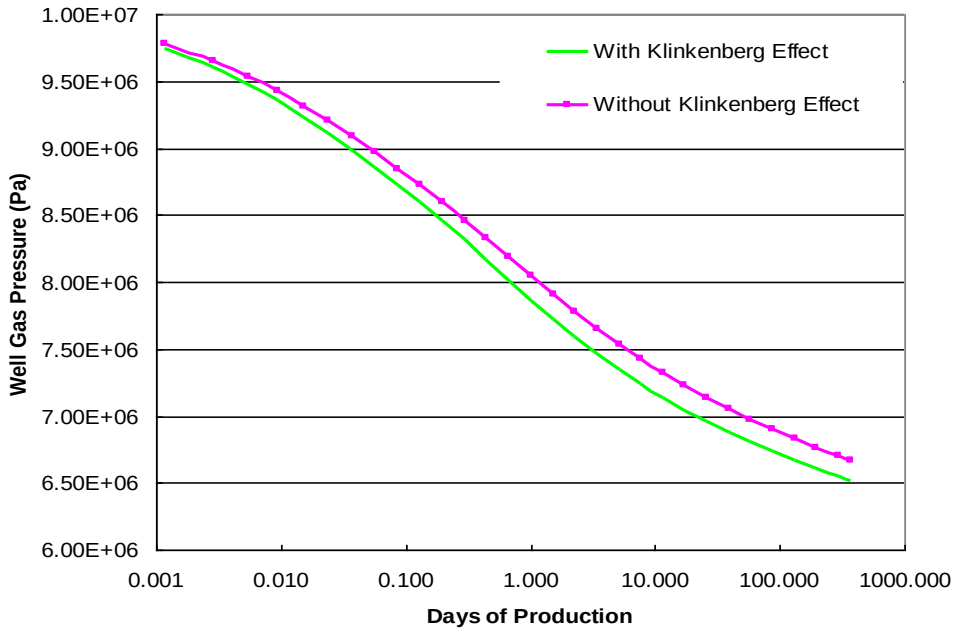

Figure 7. Changes in gas pressure at production well of flow in single-porosity media with and with out Klinkenberg effect for Problem #1.

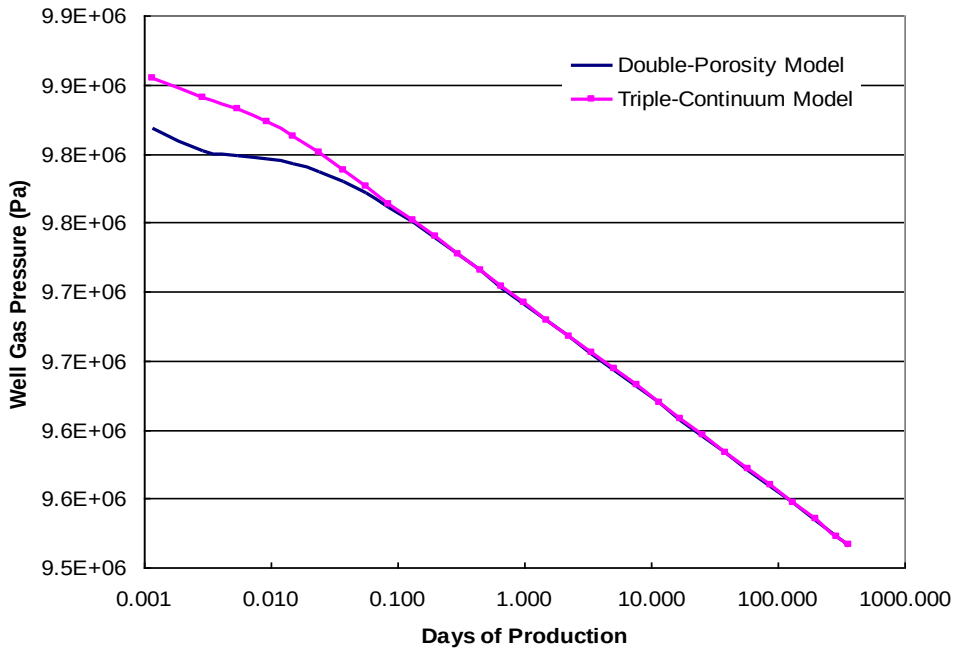

Figure 8. Changes in gas pressure at production well of flow in double-porosity and triple-continuum media for Problems #2 and 3.

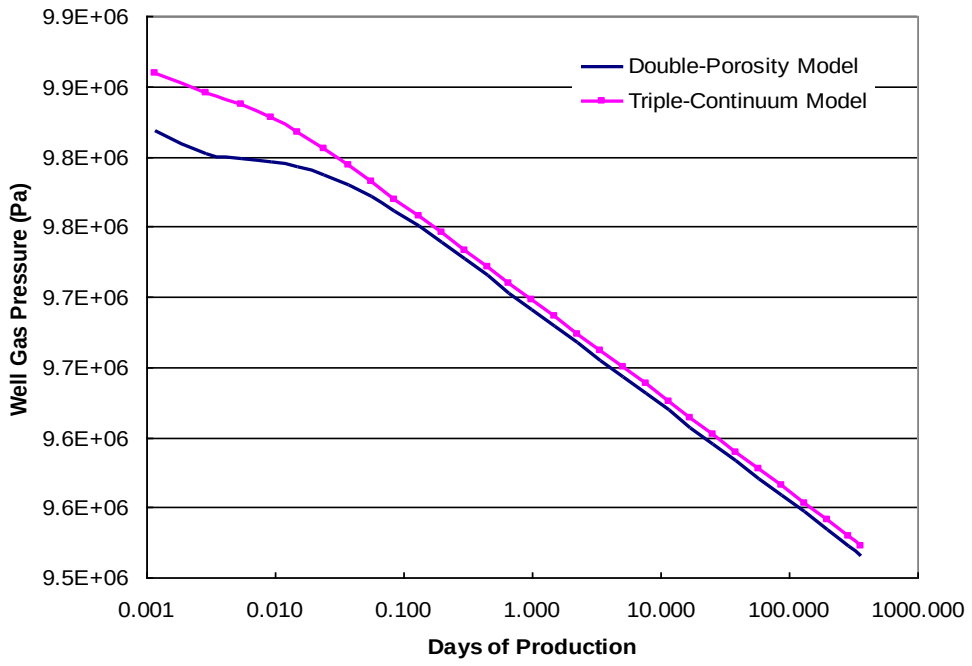

Figure 9. Changes in gas pressure at production well of flow in double-porosity and triple-continuum media for Problems #2 and 3 with large small-fracture porosity of 0.05.